ANNALS OF GEOPHYSICS, 68, 5, DM565, 2025; doi:10.4401/ag-9291
OPEN ACCESS

Joint Norwegian and Croatian temporary seismic stations deployment within AdriaArray – the CRONOS network

Josip Stipčević[*,1], Stéphane Rondenay[2], Iva Dasović[1], Dinko Šindija[1], Tena Belinić Topić[1]

(1) Department of Geophysics, Faculty of Science, University of Zagreb, Croatia
(2) Department of Earth Science, University of Bergen, Bergen, Norway

Article history: received February 14, 2025; accepted September 8, 2025

Abstract

This work presents an overview on the deployment of temporary seismic stations in the central part of the External Dinarides, aimed at enhancing our understanding of local seismic activity and tectonic processes. The deployment involved the installation of 12 new broadband stations over a period of two years. The seismometers were installed on solid building foundations lying directly on (or very close to) bedrock, providing an optimal tradeoff between ground coupling, instrument safety, and access to the power grid. Excluding one station that experienced early irreparable failure, the temporary network achieved a data recovery of the order of 87%. These temporary stations, in conjunction with several pre-existing permanent seismic instruments, allowed for the collection of high-resolution seismic data. This combined dataset was analyzed to identify seismic patterns and contribute to the broader knowledge of the Dinarides tectonic framework. The findings highlight the significance of temporary seismic networks in advancing earthquake monitoring and risk mitigation efforts in seismically active regions.

Keywords: Dinarides; seismic network; seismicity; AdriaArray;

1. Introduction

The Dinarides are a mountain chain located in the central part of the Mediterranean and are renowned for their rich geological history and complex tectonic interactions. This area serves as a boundary between several tectonic domains, including the Adriatic Microplate, which shaped the tectonic outline of the region. The Dinarides are geologically divided into the External and Internal Dinarides based on their lithological and tectonic characteristics (Fig. 1). The External Dinarides, located along the Adriatic Sea margin, are predominantly composed of Mesozoic carbonate rocks, characterized by extensive karst landscapes (Vlahović et al., 2005). In contrast, the Internal Dinarides, positioned further inland, exhibit a more complex geology with ophiolites, metamorphic rocks, and deformed sedimentary sequences indicative of their proximity to the Sava suture zone (Pamić et al., 1998; Ustaszewski et al., 2010). This division reflects the region's tectonic history, with the External Dinarides primarily

associated with the continental collision of the Adriatic Microplate, while the Internal Dinarides mark deeper structural levels of the orogenic belt resulting from the closure of the Tethys Ocean (Pamić et al., 1998; Schmid et al., 2008; Ustazewski et al., 2010).

The variations in Mohorovičić discontinuity (Moho) depth are crucial for understanding the region's tectonic evolution and geodynamic framework. The depth of the Moho beneath the Dinarides exhibits significant variability (Skoko et al., 1987; Šumanovac, 2010; Stipčević et al., 2020), reflecting the complex tectonic processes shaping the region. In the External Dinarides, near the Adriatic coast, the Moho depth is relatively shallow, ranging between 30 and 35 km, consistent with the thinner continental crust of the Adriatic microplate. Moving inland, the Moho deepens to approximately 40-45 km (and possibly over 50 km in the south Dinarides), reflecting the thicker crust associated with the orogenic wedge. Seismic studies reveal that this variability is linked to ongoing convergence and crustal shortening between the Adriatic microplate and Eurasia (e.g. Bennett et al., 2008), as well as remnants of subducted oceanic lithosphere from the closure of the Tethys Ocean (Piromallo and Morelli, 2003, Belinić et al., 2021).

The interplay between several tectonic units present in the region produces various levels of seismicity with infrequent large earthquakes (e.g. Herak et al., 1996), which can pose substantial risks to local populations and infrastructure. The most seismically active part of the region is located in the central and southern part of the External Dinarides where the seismic activity is driven by the ongoing convergence between the Adriatic Microplate and the Eurasian Plate (Handy et al., 2019). Here, the convergence results in a compressional regime characterized by reverse faulting, thrusting, and localized folding. GPS measurements indicate slow (around 3-5 mm/year) yet continuous crustal shortening, accompanied by moderate to strong seismic activity concentrated along major faults (Bennett et al., 2008) with maximum seismogenic depth closely following Moho depth variation with hypocenters mostly in the upper crust down to 20 km depth (e.g. Stipčević et al., 2020). These tectonic processes are further evidenced by uplifted Quaternary terraces, active karstic deformation, and the reactivation of older fault structures

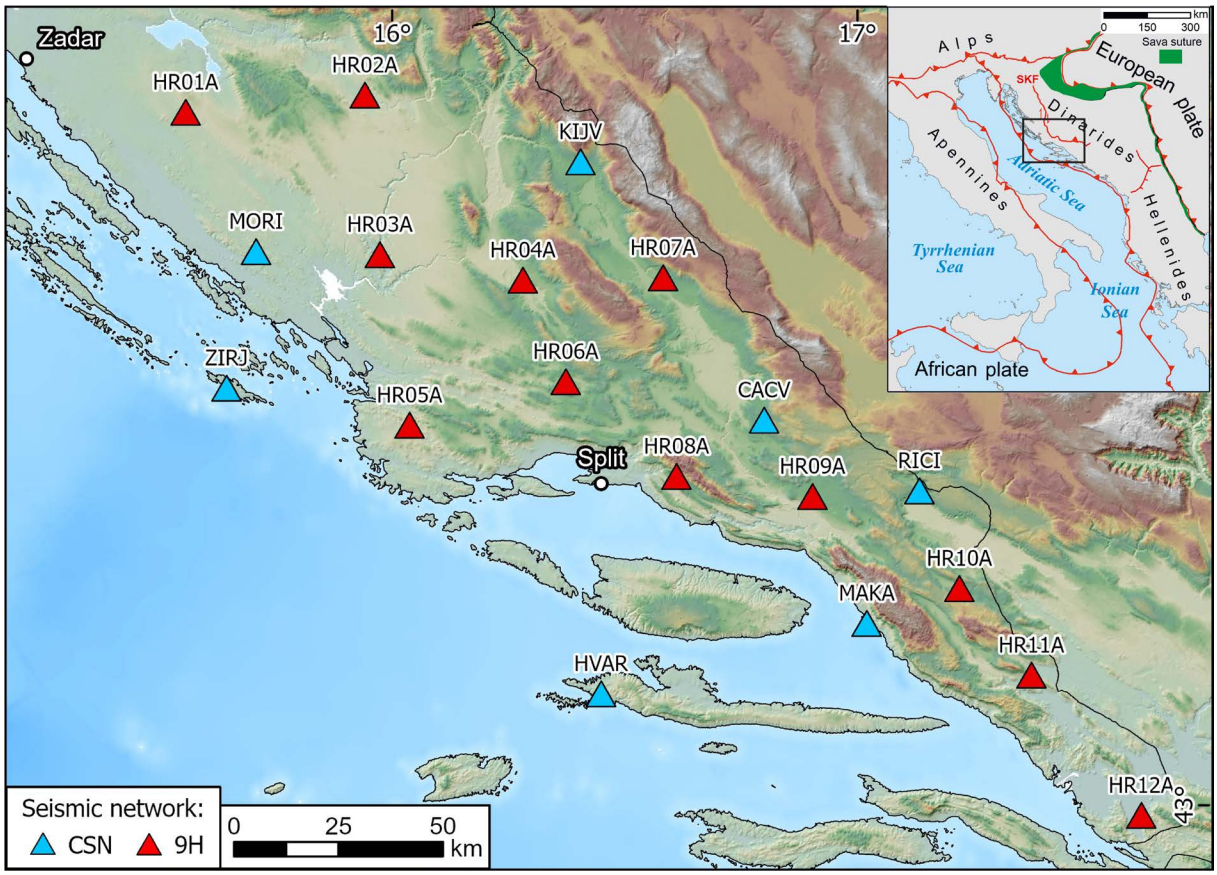

Figure 1. Seismic stations deployed during the CRONOS project (red) and stations from the Croatian permanent seismic network (blue). Inset in the upper right corner shows simplified tectonic outline of the central Mediterranean and approximate location of Internal and External Dinarides. The area shown in the main image is outlined with white rectangle. SKF denotes the Split-Karlovac Fault.

(e.g. Balling et al., 2021). Additionally, research on fault slip rates within the External Dinarides thrust-and-fold belt has provided quantitative estimates of fault movements, enhancing the understanding of seismic hazards associated with active faults in the region (Kastelic and Carafa, 2012). Such studies are crucial for assessing regional geodynamics and to estimate the occurrence of damaging earthquakes, which are indispensable for developing robust risk mitigation strategies.

The coastal area of the central External Dinarides (mostly located in Croatia with a small part of the coast in Bosnia and Herzegovina) along with the neighbouring islands (Fig 1.) is one of the Adriatic tourist hotspots with over 6 million yearly arrivals according to the Croatian Bureau of Statistics (2023). The region also hosts several larger towns and some important infrastructure facilities (e.g. ports, highways, etc.). Despite this, and despite the increasing urbanization, development and the economic significance of these factors, the current network of permanent seismic monitoring stations in the External Dinarides remains limited, hampering effective real-time monitoring and analysis needed to properly constrain the seismic hazard in the region.

To improve our understanding of subsurface structure and processes in the External Dinarides, and expand earthquake characterisation capabilities, twelve temporary broadband stations were deployed in the region over a period of two years. These, in conjunction with pre-existing permanent stations, yielded a rich dataset that is amenable to high-resolution analyses. This dataset also represents a contribution to the broader AdriaArray initiative, a pan-European cross-disciplinary scientific network that aims to investigate the tectonic processes affecting the broader central Mediterranean region (Kolínský et al., 2025). The centrepiece of the initiative is a seismic network of more than 1500 broadband stations that yields an unprecedented observational coverage of the region with an average station spacing of 50 km. Achieving such coverage requires a combination of stations from permanent national networks and dedicated temporary deployments carried out by a multitude of institutions across Europe (Kolínský et al., 2025).

In this paper, we provide a technical overview of the temporary broadband stations that were deployed in the External Dinarides and the seismic dataset that was acquired in conjunction with permanent stations. The main objective is to describe the work that was done to establish the network and provide future users with the information necessary to carry out seismic analyses with the acquired dataset. In the following section we outline the primary aims of this temporary seismic deployment along with a description of stations sites and instruments. Next, we discuss the quality and the availability of the acquired data and present some results from preliminary analyses. We conclude with a brief summary of the project outcomes and an outline of future plans.

2. The CRONOS deployment

The temporary deployment discussed in this paper took place in the central External Dinarides as part of a collaboration between the University of Zagreb and the University of Bergen within the project "*Investigation of seismically vulnerable areas in Croatia and seismic ground motion assessment* – CRONOS". This initiative was funded through the Norway Grants (Norwegian Financial Mechanism 2014-2021, the Local Development and Poverty Reduction Programme; https://projekt-cronos.hr/en/about-project/) in the wake of two devastating earthquakes that struck the city of Zagreb and the Banovina region of Croatia in 2020 (Herak et al., 2021; Herak and Herak, 2023). The overarching goal of the project was to make Croatian society more resilient to the impact of destructive earthquakes. As such, one of the aims was to explore the seismogenic sources and seismic velocity structure in Croatia, with particular focus on regions of high seismic activity such as the External Dinarides, which remain underexplored.

To address the questions raised above, and contribute to the broader AdriaArray objectives, the twelve CRONOS temporary stations were deployed in a configuration designed to provide a fairly uniform (~50 km spacing) coverage of the central External Dinarides when considered alongside the permanent stations (Fig. 1). This combined network, which includes stations from the Croatian Seismic Network (CR network), affords a dense coverage that is expected to enhance the characterization of local earthquakes and provide detailed images of the underthrusting Adriatic slab using methods such as earthquake and ambient noise tomography, full waveform tomography or receiver function analysis.

2.1 Site selections and installation

The selection process for seismic station locations in the CRONOS temporary deployment aimed to achieve an optimal spatial distribution of stations while meeting logistical and quality requirements. The primary criterion was to ensure uniform coverage across the target area, enabling effective monitoring and data acquisition for the study's objectives. To achieve this, potential station sites were strategically chosen to minimize spatial gaps, maintaining a consistent density of coverage, and taking into account the existing permanent stations from the CR network (see Fig. 1). Secondary criteria focused on practical considerations essential for station functionality and data quality. Preference was given to sites with minimal anthropogenic noise, stable ground conditions, and low seismic attenuation to maximize data integrity. Additionally, the availability of sheltered locations, such as existing buildings or enclosures, was prioritized to protect equipment from environmental elements. The presence of reliable electrical power at each site was a crucial factor to ensure uninterrupted operation of the seismic stations.

Scouting played a critical role in the location selection process by involving on-site inspections to evaluate the suitability of potential sites. During scouting, factors such as accessibility, security, local environmental conditions, and proximity to noise sources were assessed. Close communication with local stakeholders was established and maintained to secure permissions for station deployment and confirm the availability of infrastructure, including shelters and power supply. This hands-on approach allowed for the identification and resolution of potential challenges, ensuring the selected locations met both scientific and practical requirements for the temporary seismic network. Altogether, more than 50 potential locations were scouted with mixed success for some sites (e.g. HR08A, see Section 3.1) where compromises had to be made between site quality and other criteria due to lack of suitable sites. Only one seismic station was placed on a previously known location – HR05A was a previous site of the seismic station CA07A in the AlpArray-CASE experiment, in the remote village of Vinovac (Molinari et al., 2018).

The final set of locations included schools (HR01A, HR08A, HR10A), municipal buildings (HR02A, HR05A, HR06A, HR07A, HR09A, HR11A) and religious buildings (HR03A, HR04A, HR12A) – details are listed in Table 1. At all locations instruments were installed either in the basement or the ground floor, if there was no basement, of mostly one to two storey buildings (see examples in Fig. 2) with access to power supply from the electrical grid. The floor was made either of stone blocks or concrete covered by ceramic tiles. The facilities are built on hard rock or possibly on a very thin layer of soft soil on the rim of the valleys, i.e. limestone and dolomite rocks typical for the External Dinarides, therefore local site amplification was not expected. All stations were located in small settlements with less than 400 inhabitants (mostly less than 250 people), except HR11A that was placed in Vrgorac, a small town of ≈ 2100 inhabitants (Croatian Bureau of Statistics, 2022). The HR03A seismic station (Fig 2a.) is particular because it is deployed in a Franciscan monastery, a stone masonry building which partly dates to the 15th century, on Visovac island in Visovac lake formed by the course of the river Krka (National Park Krka).

The installation of the instruments was carried out by two teams in October 2022, over a four-day campaign, during which each instrument was installed at a previously determined location and connected to the local mobile data network for real-time data telemetry. The sites were periodically visited during network-wide maintenance campaigns in February-March 2023, October 2023, and February 2024. Additional site-specific visits were carried out throughout the duration of the deployment to address problems including power failure, loss of GPS lock, complete loss of communication and similar technical issues. The instruments were pulled out in October 2024.

Figure 2. Examples of site location and installation configurations for three seismic stations (rows). Pictures to the left show the station's position on Google Earth (yellow triangles). Pictures to the right display photographs of each installation site in the building that hosts the instruments. The stations are (a) HR03A in a Franciscan monastery on Visovac island in Visovac lake (National Park Krka); (b) HR08A in a small school in the mountain village Gornje Sitno, 14 km from the Split's city centre; (c) HR11A in the small town of Vrgorac.

2.2 Station configuration

Each station consisted of a broadband seismometer, a digitizer-recorder unit, a GPS antenna, a battery and charger, and a mobile router for telemetry. For the seismometers, we used a mix of Streckeisen STS-2.5 (120 s-50 Hz) and Güralp CMG-3ESPC (60 s-100 Hz) sensors. These were usually installed on concrete foundations and covered by custom-made insulation boxes made from three layers of insulation material – an outer layer made of 2.5 cm thick extruded polystyrene foam (XPS), a middle layer of 2.5 cm thick expanded polystyrene foam (EPS) and an inner layer of aluminum foil (Fig. 2). Each station was equipped with an EarthData EDR-210 digitizer-recorder unit. The sampling rate was set at 100 Hz everywhere. Data were recorded on local SSD drives and transferred in real time via SeedLink protocol to the UIB-NORSAR EIDA node (Network code 9H). The recording instruments, router and power supplies were housed in the station carrying cases (blue boxes in Fig. 2). Table 1 provides an overview of the seismometers used at each site, along with geographical coordinates and a summary of known timing issues.

Various technical issues occurred at several stations over the course of the experiments, including loss of power to the instruments (due to accidental power disconnection, power surge, lightning strike), malfunctioning GPS, and malfunctioning recorder, leading to an overall data recovery of ~87% excluding station HR05A. The station HR05A was struck by lightning early on during the experiment and could not be reinstalled because the instruments were damaged beyond repair. More details about these technical issues are given in Section 3.2.

Table 1. Locations (geographical coordinates and elevation above sea level) and general information (start time and end time, type of the seismometer, known timing issues) for all temporary stations in the 9H seismic network. The two types of seismometers are Streckeisen STS-2.5 (120 s-50 Hz) and Güralp CMG-3ESPC (60 s-100 Hz).

Station	Latitude (°N)	Longitude (°E)	Elevation (m)	Start	End	Seismometer	No GPS time
HR01A	44.08	15.56	214	13.10.22	30.09.24	STS-2.5	13.10.22-20.10.22
HR02A	44.11	15.94	126	14.10.22	30.09.24	3ESPC	—
HR03A	43.86	15.97	41	14.10.22	01.10.24	STS-2.5	14.10.22-14.12.22
HR04A	43.82	16.28	314	15.10.22	01.10.24	3ESPC	—
HR05A	43.59	16.06	189	15.10.22	03.12.22	3ESPC	—
HR06A	43.66	16.37	342	15.10.22	16.05.24	STS-2.5	—
HR07A	43.83	16.58	419	17.10.22	02.10.24	STS-2.5	—
HR08A	43.52	16.61	576	17.10.22	02.10.24	3ESPC	—
HR09A	43.49	16.90	403	18.10.22	28.06.24	STS-2.5	—
HR10A	43.34	17.22	354	18.10.22	03.07.24	3ESPC	—
HR11A	43.21	17.37	200	19.10.22	03.10.24	3ESPC	—
HR12A	42.99	17.61	23	19.10.22	03.10.24	STS-2.5	—

3. Data

3.1 Data quality

In order to check the general quality of recordings for each station we calculated the seismic power spectral density (PSD) using the direct Fourier method (Cooley and Tukey, 1965), implemented with the ObsPy software package (Krischer et al., 2015) and following the methodology of McNamara and Buland (2004). The probability density functions (PDFs) generated from the PSD provide valuable insights into ambient noise conditions by highlighting noise levels with high occurrence probabilities. PDFs serve as a standard tool for assessing background Earth noise at each site, as well as for identifying artifacts related to station operations and occasional cultural noise.

To evaluate the quality of stations within the 9H network, we computed the median PSD for each station and compared them with the New High Noise Model (NHNM) curves (Peterson, 1993) and the AdriaArray noise requirement

curves (AANM). The AdriaArray noise criteria, aligned with those of AlpArray (Molinari et al., 2018), specify that noise levels at each station must be at least 20 dB lower than the NHNM for most components within the 1-10 Hz frequency range. For horizontal components, noise levels need to be 10 dB below the NHNM due to generally higher noise on these components, arising from factors such as atmospheric pressure fluctuations and surface tilt, particularly in long-period measurements. A summary of the PSD medians for the CRONOS temporary installations is shown in Fig. 4, which includes both the vertical and E-W components (for brevity, we only show E-W components because they are very similar to N-S components).

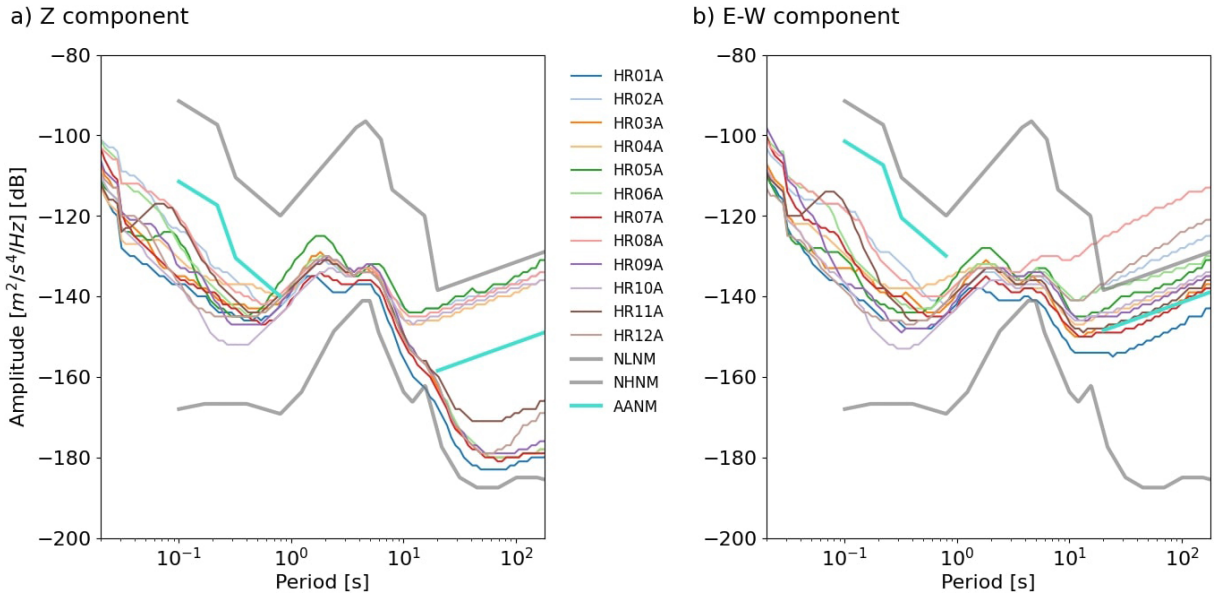

Figure 3. Median power spectral density (PSD) curves for all operating CRONOS stations from October 2022 to October 2024. Each line represents an individual station's PSD: (a) vertical component and (b) east-west horizontal component. Thick light grey lines indicate the New High Noise Model (NHNM) and New Low Noise Model (NLNM), while the thick teal line represents the AdriaArray noise level requirement (AANM), note that AANM was not defined between periods 1 to 10 s.

For short periods ($T < 1$ s), all stations meet the AdriaArray noise level requirements for both components. At longer periods ($T > 10$ s), vertical components show varied noise levels: seven stations exhibit much lower noise than the AANM requirements, while five are below the NHNM but above the AANM. Horizontal components at long periods show even higher noise levels: only two stations meet the AANM, seven fall below the NHNM, and three do not meet the NHNM. Long-period components are influenced by atmospheric pressure changes, wind (e.g., Webb, 2002), building warping, temperature fluctuations, and sensor-to-ground coupling. High noise levels at certain sites are linked to specific conditions, including foot traffic in buildings (especially during summer) and coastal locations. Weather variations, like storms and winds further contribute. Additionally, thermal insulation, particularly against temperature and pressure changes, plays an important role; more solid insulation could improve performance. For stations with higher noise levels, such as HR08A and HR02A, site conditions are the primary contributing factor.

The probability density functions for the three components of all CRONOS stations are presented in Appendix A (Figs. A1-A3). In Fig. 5, we present examples of PDFs for three stations in the 9H network, representing low, high and average noise levels for vertical and E-W components (N-S components are very similar to E-W components). Station HR03A (Fig. 5a) exhibits some of the lowest noise levels on both components. Located in the Franciscan monastery on the island of Visovac in Krka National Park (Fig. 2), the site remains quiet during the winter and at night, as only a few monks reside there. However, in the summer, the monastery becomes a popular tourist destination, leading to an increase in noise levels. The effect of foot traffic is visible in the long-period horizontal components, but the station still meets the AANM requirements, with overall noise levels remaining very good.

Station HR08A (Fig. 5b) exhibits the highest noise levels on both components. It is located in the basement of a two-story stone masonry (Fig. 2) in the village center, which previously was used as a small branch of Primary School Žrnovica but is now empty. The station is affected by a combination of high anthropogenic noise levels in the village and a building foundation that may be partially hollowed. For shorter periods, both components fall below the AANM levels, but at longer periods, the vertical component is below the NHNM but still above the AANM. The horizontal component exceeds the NHNM.

Station HR11A (Fig. 5c) shows average noise levels on both components. Located in the basement of a one-storey building within a cemetery and owned by the Vrgorac municipality, the vertical component remains below the AANM levels across all periods. For the horizontal component, noise is below the AANM levels for shorter periods, but at longer periods, it falls below the NHNM and above the AANM, resulting in overall good noise levels, especially considering the presence of people working there and the close proximity to a town of 2100 inhabitants.

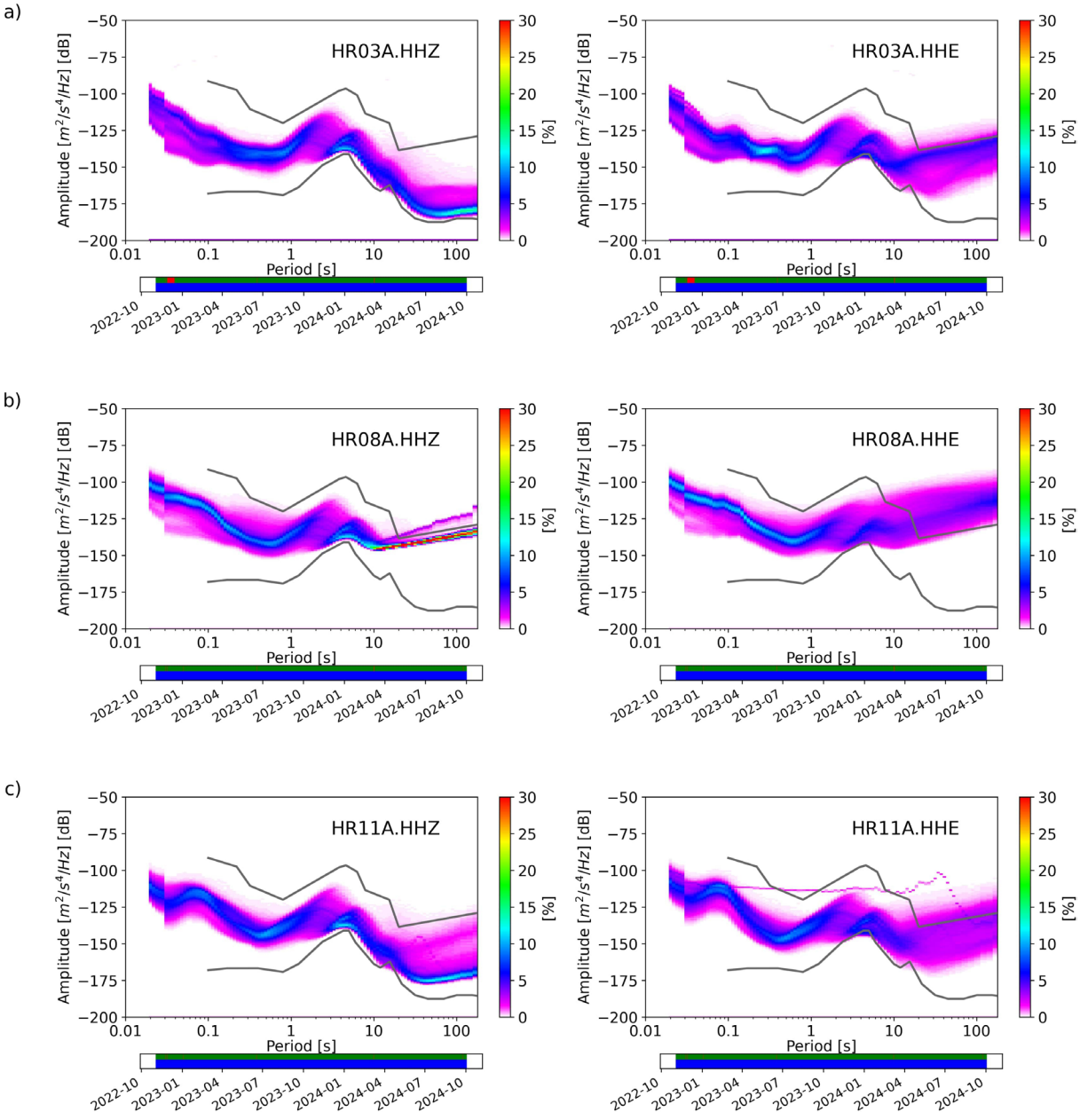

Figure 4. Probability density functions of vertical (left) and E-W (right) components for three CRONOS temporary stations: (a) HR03A, (b) HR08A and (c) HR11A. The thick grey lines correspond to the NHNM and NLNM models.

3.2 Data completeness and data transmission

At the time of writing, nearly two years of data have been collected from most of the CRONOS temporary seismic stations, primarily through real-time communications. The data availability for the 9H stations is of the order of 87% (excluding the station HR05A which recorded almost no data) as can be seen in Fig. 6. Some gaps could be filled after the data were manually collected and stored in the database. However, large gaps after installation and before March 2023 are not recoverable due to interruptions in station operation, such as power supply issues and digitizer malfunctions, which we will discuss in more detail below.

Several stations encountered issues that affected data continuity and the station with the shortest data recorded was station HR05A. Station HR05A experienced a complete equipment failure in December 2022, when the sensor, digitizer, and breakout box burnt out in a charger explosion, leading to the permanent removal of equipment only a few months after installation. Station HR03A experienced issues with the GPS antenna, impacting data accuracy until the problem was resolved in December 2022. The most common problems we encountered were digitizer issues, usually occurring after power-cuts. Station HR01A experienced issues in the second part of 2023 due to a faulty cable connecting the instrument and digitizer. Similarly, station HR10A initially suffered a malfunctioning digitizer due to a power outage at the station, which, after being replaced on March 1, allowed the station to resume normal operations. Later, after a power outage on June 25, 2023, digitizer was stuck in a rebooting loop every ten minutes and couldn't mount parts of the internal drive which required firmware update and formatting of the internal flash drive. Station HR07A suffered from a faulty power cable, limiting its data collection to only 30 minutes from installation until the cable was replaced on March 3, 2023. In October 2023, an issue with both digitizer and router at station HR09A occurred which was fixed with the replacement of both components. Lastly, recording ended prematurely by 3-4 months prior to pullout at three sites (HR06A, HR09A, HR10A) due to digitizer malfunction.

Despite these challenges, most stations managed to capture continuous data throughout the two years. Seven stations remained operational at all times. Some stations relied on variable mobile network coverage,

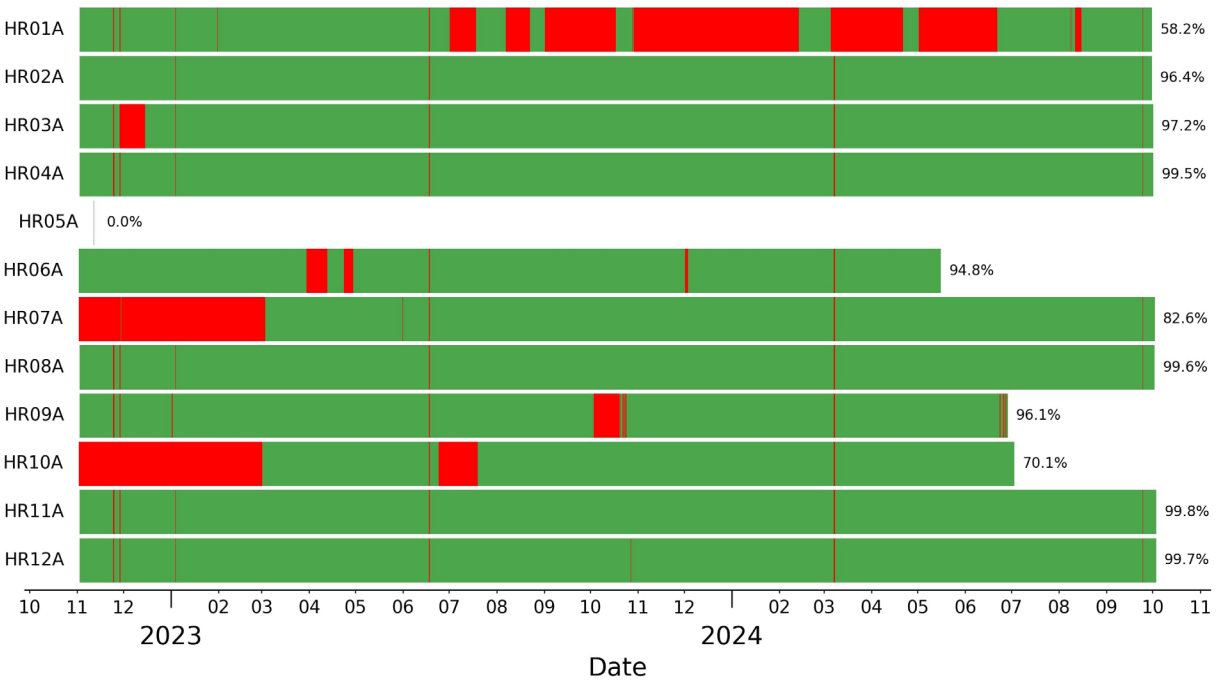

Figure 5. Data availability from real-time communication for the twelve temporary CRONOS stations (9H) from their installation dates through October 2024. Data gaps are continuously filled as they are manually retrieved and added to the database. Due to operational interruptions, large, unrecoverable gaps before March 2023 are present at stations HR10A and HR07A. Station HR05A ceased operation in December 2022. See main text for details. Recording at stations HR06A, HR09A and HR10A ended prematurely due to digitizer malfunction – if one considers actual station pullout time in October 2024 their effective data recovery rates are approximately 77%, 84% and 61%, respectively.

but the connection bandwidth was generally acceptable. The final data gaps were filled at the project's conclusion in October 2024.

4. Results – examples

4.1 Local and Regional earthquakes

Figure 7 shows the real-time waveforms recorded by the 9H stations for two earthquakes: a local earthquake (M4.3) that occurred near the town of Metković in southern Croatia on 23 September 2023 at 17:01:34 UTC, and a regional earthquake (M7.8) that took place in Turkey on 6 February 2023 at 01:17:36 UTC. The epicenter of the local earthquake was located just 8 km from the CRONOS station HR12A. Due to its proximity to the network, the local event was recorded with excellent clarity, with well-defined P and S wave arrivals (Fig. 7b), which are crucial for accurate phase picking and event characterization. In contrast, the regional earthquake in Turkey generated strong and prolonged seismic signals across the network (Fig. 7d). Despite the relatively large epicentral distance (D ~1880 km), the stations recorded the different seismic phases clearly, demonstrating the 9H network's ability to capture both local and distant events. The differences in amplitude, frequency content and wave propagation characteristics between the two events show the importance of having a dense network of seismic broadband stations capable of detecting a wide range of seismic sources. The high-quality recordings of both earthquakes underscore the effectiveness of the CRONOS experiment in monitoring seismic activity. Detecting and analyzing local earthquakes in real-time

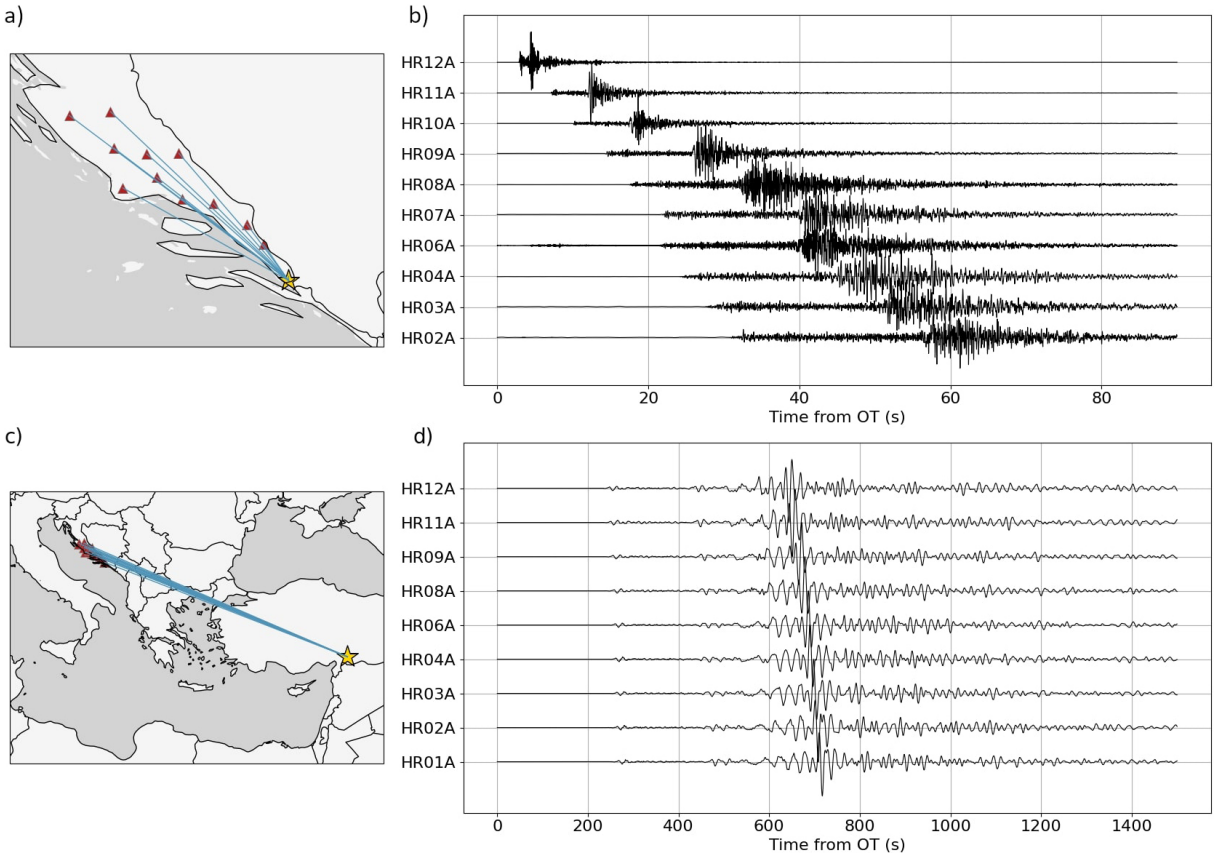

Figure 6. Examples of waveforms recorded by the CRONOS temporary stations (marked with red triangles) and drawn based on the earthquake origin time (OT). Epicenters are marked with a yellow star, while blue lines indicate ray paths. (a) Location of the M4.3 local earthquake that occurred on 23 September 2023 in Bosnia and Herzegovina, near the border with Croatia; (b) Associated waveforms for the local earthquake; (c) Location of the M7.8 regional earthquake that occurred on 6 February 2023 in Turkey (D ~1880 km); (d) Recorded seismograms for the Turkish earthquake shown in panel (c).

is especially valuable for understanding regional seismicity and assessing potential hazards. With its dense station coverage, the 9H network can capture even smaller seismic events that might otherwise go unnoticed. We further enhanced this capability by applying machine learning techniques for phase detection, improving the accuracy and completeness of seismic monitoring.

4.2 Local seismicity monitoring during the experiment

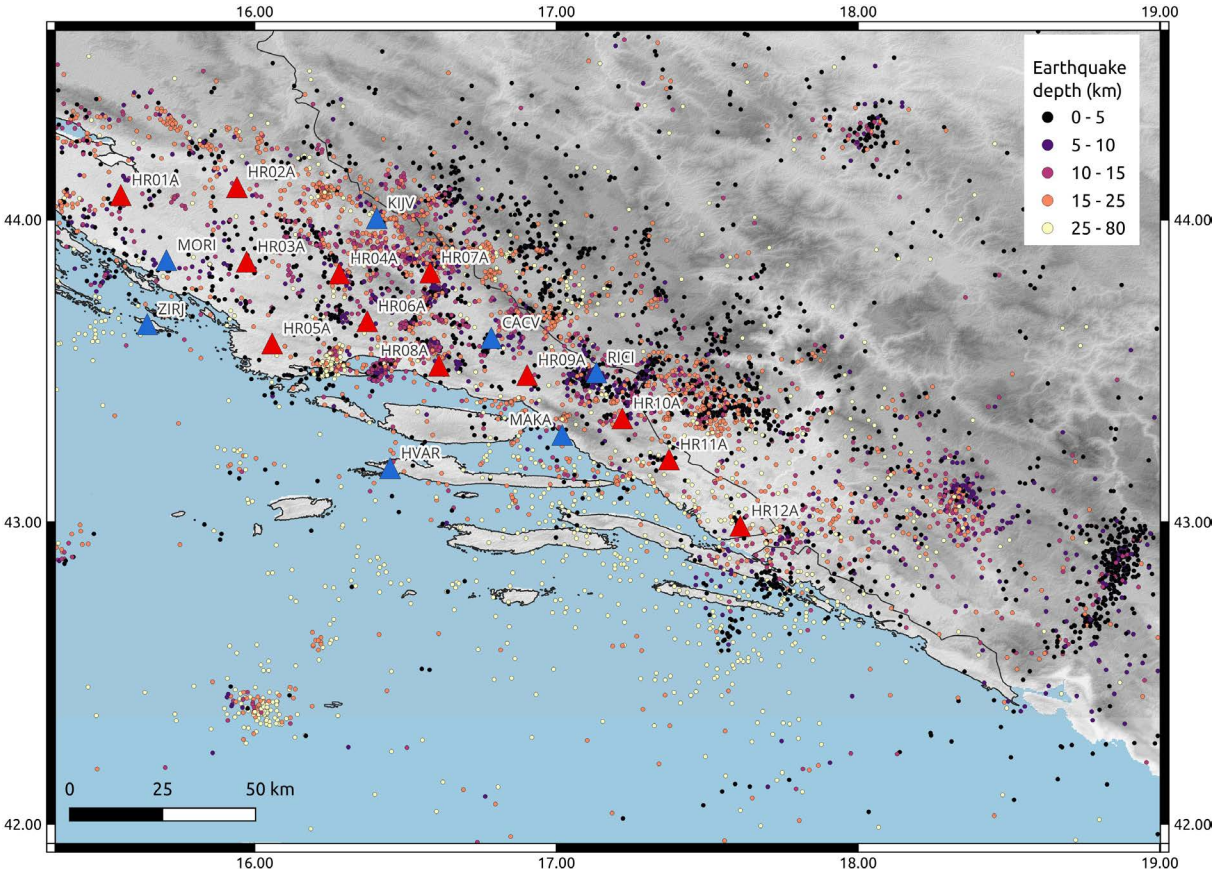

Figure 7. Earthquake locations in the preliminary CRONOS catalogue for the period November 2022-August 2024. Depth for each earthquake is color coded as shown in color scale. Triangles represent seismic stations deployed during the CRONOS project (red) and stations from the Croatian permanent seismic network (blue).

For almost the complete time window of the CRONOS experiment (November 1, 2022-August 30, 2024), we conducted seismic phase detection and generated a preliminary earthquake catalog using automated machine learning methods. We employed EQTransformer (Mousavi et al., 2020) trained on the INSTANCE training dataset (Michelini et al., 2021) for initial earthquake phase detection through the Seisbench toolbox (Woolam et al., 2022). The P and S wave probability thresholds were defined at 0.05, indicating that any pick with a confidence value above this threshold was treated as a respective phase arrival. EQTransformer analyzes 60-second data segments with adjustable overlapping windows, and as demonstrated by Pita-Sllim et al. (2023), the accuracy of P and S phase detections is highly sensitive to the start time of the phases within these segments. To mitigate this, we used a window overlap of 50 seconds, aiming to optimize the balance between detection rates and minimizing false positives, in conjunction with the P and S probability thresholds (Pita-Sllim et al., 2023). Although the low threshold values for P and S phases increase the likelihood of false positive detections, these are later filtered out through the association and relocation processes. The detection is done on all of the stations of the 9H network and on seven stations (KIJV, MORI, ZIRJ, CACV, RICI, MAKA, HVAR) from the permanent CR Network (Fig. 8). The aforementioned parameters were discussed and agreed upon during meetings of the 'Machine Learning for Seismicity Detection and Location & Crowd Processing' subgroup, which is part of the AdriaArray Seismicity Collaborative Research Group,

in order to create a uniform seismic catalog across the complete AdriaArray deployment. For phase association, we use the PyOcto (Munchmeyer, 2024) phase associator based on space-time partitioning. The preliminary event locations are calculated using a homogeneous halfspace – this assumption should work in the first iteration as it is sufficient for regions with shallow seismicity. The final step in the location process is done with NonLinLoc (Lomax et al., 2000), for which we used a 1D velocity model for the central Adriatic region from Latečki (2024). Our analysis detected a total of 2,956,559 seismic phases, consisting of 2,129,757 P phases and 826,802 S phases. Of these, 397,367 P and 114,732 S phases were observed on permanent CR network stations while 1,732,390 P and 712,070 S phases were detected on 9H network stations. To associate seismic phases with earthquake events using PyOcto, we applied a minimum requirement of 12 phases per event, resulting in a total of 146,712 "valid" picks (78,833 P and 67,879 S phases). Notably, 63% of associated picks are attributed to the 9H network with 49,179 P and 43,320 S phases. After the association and relocation process, our preliminary seismic catalog consists of 7,749 events (Fig. 8). Total number of earthquakes per month and the cumulative number of earthquakes versus time for our provisional catalog are shown in Fig. 9. We can see there is no significant seismicity change in seismic activity during this analyzed period.

For this preliminary catalogue, we did not perform manual quality control or cross-checking against an existing manually picked catalogues. However, previous work in the nearby Petrinja region using an equivalent workflow has shown up to a 95% match with detailed manual catalogue, with accuracy improving significantly when the network was densified (Šindija et al., 2025). Further, by using minimum requirement of 12 phases per event we reduced the likelihood of false positive detections in this preliminary catalogue. This result can act as an initial stage for the creation of the final catalogue after integration of the remaining stations in the CR network and additional stations from the temporary Y5 network (Obermann et al., 2022) in the neighboring Bosnia and Herzegovina thereby improving the location accuracy.

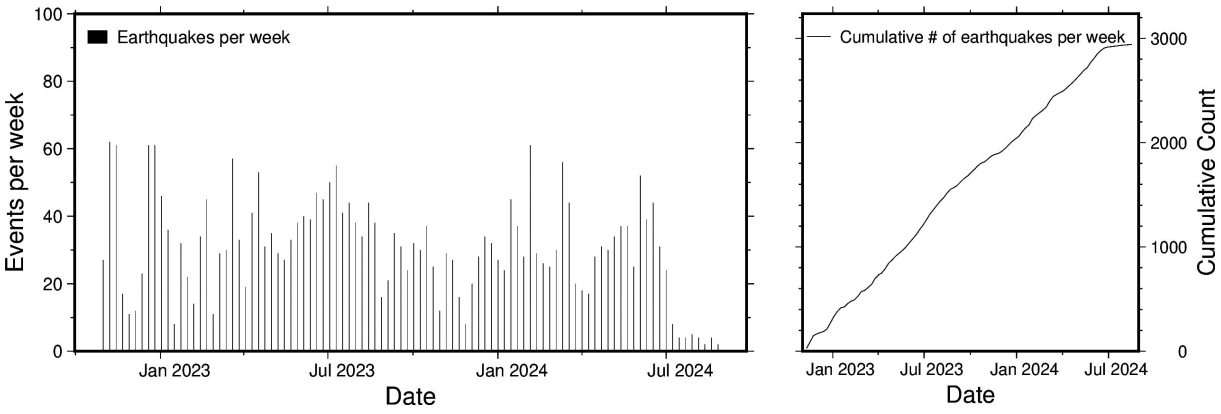

Figure 8. Total number (left) and cumulative number (right) of earthquakes per week for our provisional catalog during the analyzed period (November 1, 2022-August 30, 2024)

5. Concluding remarks

The twelve temporary seismographs of the CRONOS project have significantly improved the seismic station coverage in a part of the External Dinarides that had previously been sparsely instrumented. Along with the existing permanent stations of the Croatian Seismograph Network, they have yielded an enhanced dataset that allows for an unprecedented level of earthquake detections in the region, utilizing both traditional and state-of-the-art machine learning-based approaches. This improved detection capability, though limited to the two-year deployment period, has resulted in a high-resolution earthquake catalogue that now serves as a valuable resource for better constraining seismically active areas. These insights can be instrumental in seismic hazard assessments, helping to identify focus areas in future risk mitigation strategies.

Beyond immediate applications, the CRONOS dataset represents an important contribution to the broader AdriaArray initiative, which aims to enhance seismic imaging and geodynamic understanding across the central Mediterranean and adjacent regions. The expanded seismic coverage in the External Dinarides offers a unique

opportunity to address fundamental questions about the region's tectonic evolution, including the nature of active faulting, crustal deformation patterns, and the role of inherited structures in present-day seismicity. Additionally, the dataset will help improve tomographic models of the lithosphere, shedding light on the deep structure of the Adriatic microplate and its interactions with surrounding tectonic units.

Future research efforts will build upon these findings by integrating the CRONOS dataset with other regional and international seismic networks, fostering collaborations aimed at advancing our understanding of seismic hazards and geodynamic processes in the broader Mediterranean region. The temporary nature of the deployment underscores the importance of continued monitoring efforts and the potential benefits of expanding permanent seismic station coverage in this seismically active area.

Data availability statement. Waveform data from the permanent station with network code CR are available through ORFEUS EIDA. Data from temporary stations of the CRONOS project with network code 9H are accessible through the UIB-NORSAR ORFEUS EIDA node (www.orfeus-eu.org/data/eida/nodes/UIB_NORSAR/) to the AdriaArray Seismology Group participants. The rolling embargo allows this data to be publicly available two years after its acquisition. Data from all AdriaArray temporary stations are, however, immediately available for seismological observatories with monitoring and alerting duties within the AdriaArray region.

Acknowledgements. This study has been fully supported by the project "Investigation of seismically vulnerable areas in Croatia and seismic ground motion assessment – CRONOS" funded by the Norwegian Grants (Norwegian Financial Mechanism 2014-2021, grant 04-UBS-U-0002/22-90). The seismic instruments used for the CRONOS temporary network were leased from the Norwegian Pool of Advanced Broad-Band Seismic Instruments (NFR Research Infrastructure Grant 208293), which is coordinated and maintained by NORSAR. We thank Morten Sickel and Jon Magnus Christensen at NORSAR for their help preparing the instruments, instruments troubleshooting and transport logistics. We are indebted to the municipalities of Ervenik, Ružić, Marina, Klis, Hrvace, Šestanovac and Zažablje, the town of Vrgorac, public elementary schools in Benkovac, Žrnovnica and Zagvozd and to the Franciscan Monastery of Visovac that allowed us to install stations in their properties and looked after them during the project. We also thank all the personnel involved in the installation/servicing of stations and related logistics, as well as data telemetry and archiving: Helena Latečki, Lucija Golub, Felix Halpaap, Marin Sečanj, Lars Ottemöller, Øyvind Natvik and Jan Michalek.

References

Balling, P., C. Grützner, B. Tomljenović, W. Spakman and K. Ustaszewski (2021). Post-collisional mantle delamination in the Dinarides implied from staircases of Oligo-Miocene uplifted marine terraces, Sci Rep., 11, 2685, doi:10.1038/s41598-021-81561-5

Belinić, T., P. Kolínský, J. Stipčević and the AlpArray Working Group (2021). Shear-wave velocity structure beneath the Dinarides from the inversion of Rayleigh-wave dispersion, Earth and Planet. Sci. Lett., 555, 116686, doi:10.1016/j.epsl.2020.116686.

Bennett, R. A., S. Hreinsdóttir, G. Buble, T. Bašić, Ž. Bačić et al. (2008). Eocene to present subduction of southern Adria mantle lithosphere beneath the Dinarides, Geology, 36, 1, 3-6, doi:10.1130/G24136A.1

Cooley, J. W. and J. W. Tukey (1965). An algorithm for the machine calculation of complex Fourier series, Math. Comput., 19, 297-301, doi:10.1090/S0025-5718-1965-0178586-1.

CR – University of Zagreb. (2001). Croatian Seismograph Network [Data set]. International Federation of Digital Seismograph Networks, doi:10.7914/SN/CR.

Croatian Bureau of Statistics (2022). Census of Population, Households and Dwellings in the Republic of Croatia in 2021 – Population by Settlements, https://dzs.gov.hr/u-fokusu/popis-2021/popisni-upitnik/english/results/1501. Accessed on 29 January 2025.

Croatian Bureau of Statistics (2023). Tourist Arrivals and Nights in Commercial Accommodation, 2023, https://podaci.dzs.hr/2023/en/58170. Accessed on 2 February 2025.

Handy, M. R., J. Giese, S. M. Schmid, J. Pleuger et al. (2019). Coupled crust-mantle response to slab tearing, bending, and rollback along the Dinaride-Hellenide orogen, Tectonics, 38, 2803-2828, https://doi.org/10.1029/2019TC005524.

Herak, M., D. Herak and S. Markušić (1996). Revision of the earthquake catalog and seismicity of Croatia, 1908-1992. Terra Nova, 8, 86-94, doi:10.1111/j.1365-3121.1996.tb00728.x.

Herak, M., D. Herak and N. Orlić (2021). Properties of the Zagreb 22 March 2020 earthquake sequence – analyses of the full year of aftershock recording, Geofizika, 38, 2, 93-116, doi:10.15233/gfz.2021.38.6.

Herak, M. and D. Herak (2023). Properties of the Petrinja (Croatia) earthquake sequence of 2020-2021 – Results of seismological research for the first six months of activity, Tectonophysics, 858, 229885, doi:10.1016/j.tecto.2023.229885.

Kastelić, V. and M. M. C. Carafa (2012). Fault slip rates for the active External Dinarides thrust-and-fold belt, Tectonics, 31, TC3019, doi:10.1029/2011TC003022

Krischer, L., T. Megies, R. Barsch, M. Beyreuther et al. (2015). ObsPy: A bridge for seismology into the scientific Python ecosystem, Computat. Sci. Discov., 8, 014003, doi:10.1088/1749-4699/8/1/014003.

Kolínský, P., T. Meier, M. Agius, A. Bijedić et al. (2025). AdriaArray – a Passive Seismic Experiment to Study Structure, Geodynamics and Geohazards of the Adriatic Plate, Ann. Geophys., 68, this issue.

Latečki, H., (2024). Seismic shaking scenarios for the wider Dubrovnik area, (Doctoral dissertation), University of Zagreb. (in Croatian).

Lomax, A., J. Virieux, P. Volant, C. Berge-Thierry (2000). Probabilistic Earthquake Location in 3D and Layered Models. In: Thurber, C. H., Rabinowitz, N. (eds) Advances in Seismic Event Location. Modern Approaches in Geophysics,18, Springer, Dordrecht, doi:10.1007/978-94-015-9536-0_5.

McNamara, D. E. and R. P. Buland (2004). Ambient noise levels in the continental United States, Bulletin of the Seismological Society of America, 94, 4, 1517-1527, https://doi.org/10.1785/012003001.

Michelini, A., S. Cianetti, S. Gaviano, C. Giunchi et al. (2021). INSTANCE – the Italian seismic dataset for machine learning, Earth Syst. Sci. Data, 13, 12, 5509-5544, doi:10.5194/essd-13-5509-2021.

Molinari, I., I. Dasović, J. Stipčević, V. Šipka et al. (2018). Investigation of the central Adriatic lithosphere structure with the AlpArray-CASE seismic experiment, Geofizika, 35, 2, 103-128, doi:10.15233/gfz.2018.35.6.

Mousavi, S. M., W. L. Ellsworth, W. Zhu et al. (2020). Earthquake transformer – an attentive deep-learning model for simultaneous earthquake detection and phase picking, Nat. Commun. 11, 3952. https://doi.org/10.1038/s41467-020-17591-w.

Münchmeyer, J. (2024). PyOcto: A high-throughput seismic phase associator, Seismica, 3, 1, doi:10.26443/seismica.v3i1.1130

Obermann, A., D. Jozinović, S. Cvijić, A. Krehić and Swiss Seismological Service (SED) at ETH Zurich (2022). Swiss Contribution to AdriaArray Temporary Network. ETH Zurich, doi:10.12686/SED/NETWORKS/Y5.

Pamić, J., I. Gušić and V. Jelaska (1998). Geodynamic evolution of the Central Dinarides, Tectonophysics, 297, 1-4, 251-268, doi:10.1016/S0040-1951(98)00171-1.

Peterson, J. (1993). Observations and modeling of seismic background noise, USGS Open-File report, 93-322, doi:10.3133/ofr93322.

Piromallo, C. and A. Morelli (2003). P wave tomography of the mantle under the Alpine-Mediterranean area, J. Geophys. Res., 108, B2, 2065, doi:10.1029/2002JB001757.

Pita-Sllim, O., C. J. Chamberlain, J. Townend and E. Warren-Smith (2023). Parametric testing of EQTransformer's performance against a high-quality, manually picked catalog for reliable and accurate seismic phase picking, The Seismic Record, 3, 4, 332-341, doi:10.1785/0320230024.

Schmid, S. M., D. Bernoulli, B. Fügenschuh, L. Matenco et al. (2008). The Alpine-Carpathian-Dinaridic orogenic system: Correlation and evolution of tectonic units, Swiss J. Geosci., 101, 1, 139-183, doi:10.1007/s00015-008-1247-3.

Šindija, D., M. Mustać, G. Hetényi and J. Stipčević (2025). Enhanced view of the Mw 6.4 Petrinja earthquake sequence (2020-2022) using deep learning, ESS Open Archive, June 13, 2025, doi:10.22541/essoar.174982734.45695605/v1.

Skoko, D., E. Prelogović and B. Aljinović (1987). Geological structure of the Earth's crust above the Moho discontinuity in Yugoslavia, Geophys. J. of the Royal Astronomical Society, 89, 379-382. doi:10.1111/j.1365-246X.1987.tb04434.x.

Šumanovac, F. (2010). Lithosphere structure at the contact of the Adriatic microplate and the Pannonian segment based on the gravity modeling, Tectonophysics, 485, 1-4, 94-106, doi:10.1016/j.tecto.2009.12.005.

Stipčević, J., H. Tkalčić, M. Herak and S. Markušić (2011). Crustal and uppermost mantle structure beneath the External Dinarides, Croatia, determined from teleseismic receiver functions, Geophys. J. Int., 185, 1103-1119, doi:10.1111/j.1365-246X.2011.05004.x.

Stipčević, J., M. Herak, I. Molinari, I. Dasović, H. Tkalčić and A. Gosar (2020). Crustal thickness beneath the Dinarides and surrounding areas from receiver functions, Tectonics, 37, doi:10.1029/2019TC005872.

Ustaszewski, K., A. Kounov, S. M. Schmid, U. Schaltegger et al. (2010). Evolution of the Adria-Europe plate boundary in the northern Dinarides: From continent-continent collision to back-arc extension, Tectonics, 29, 6, TC6017, doi:10.1029/2010TC002668.

Vlahović, I., J. Tišljar, I. Velić and D. Matičec (2005). Evolution of the Adriatic Carbonate Platform: Palaeogeography, main events and depositional dynamics, Palaeogeogr., Palaeoclimat., Palaeoecol., 220, 333-360, doi:10.1016/j.palaeo.2005.01.011.

Webb, S. C. (2002). Seismic Noise on Land and on the Sea Floor, in International Hand-book on Earthquake and Engineering Seismology, Volume 8, Part A edited by Lee, W. H. K., Kanamori, H., Jennings, P.C. and C. Kisslinger, Academic Press, Amsterdam, 305-318, ISSN:0074-6142, https://doi.org/10.1016/S0074-6142(02)80222-4.

Woollam, J., J. Münchmeyer, F. Tilmann, F., A. Rietbrock, D. Lange et al. (2022). SeisBench – A toolbox for machine learning in seismology, Seismol. Res. Lett., 93, 3, 1695-1709, doi:10.1785/0220210324.

Appendix A. Probability density functions

Here we present probability density functions for the vertical, east-west (E-W), and north-south (N-S) components at twelve CRONOS temporary stations. These PDFs are compared against the New High Noise Model (NHNM) and the New Low Noise Model (NLNM). The figures are referenced in the main text of the paper.

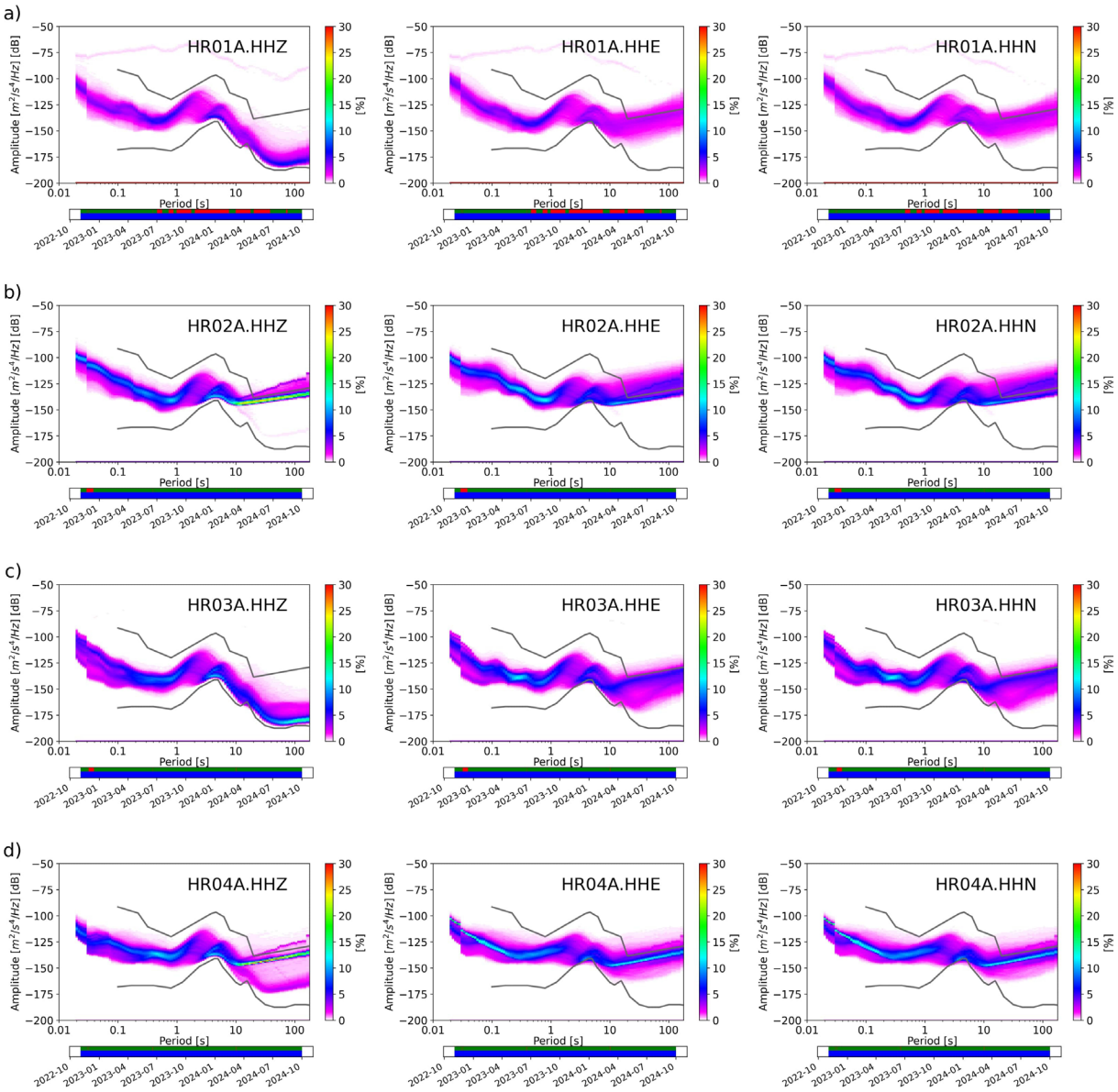

Figure A1. Probability density functions of vertical (left), E-W (middle), and N-S (right) components for four CRONOS temporary stations: (a) HR01A, (b) HR02A, (c) HR03A and (d) HR04A. The thick grey lines correspond to the NHNM and NLNM models.

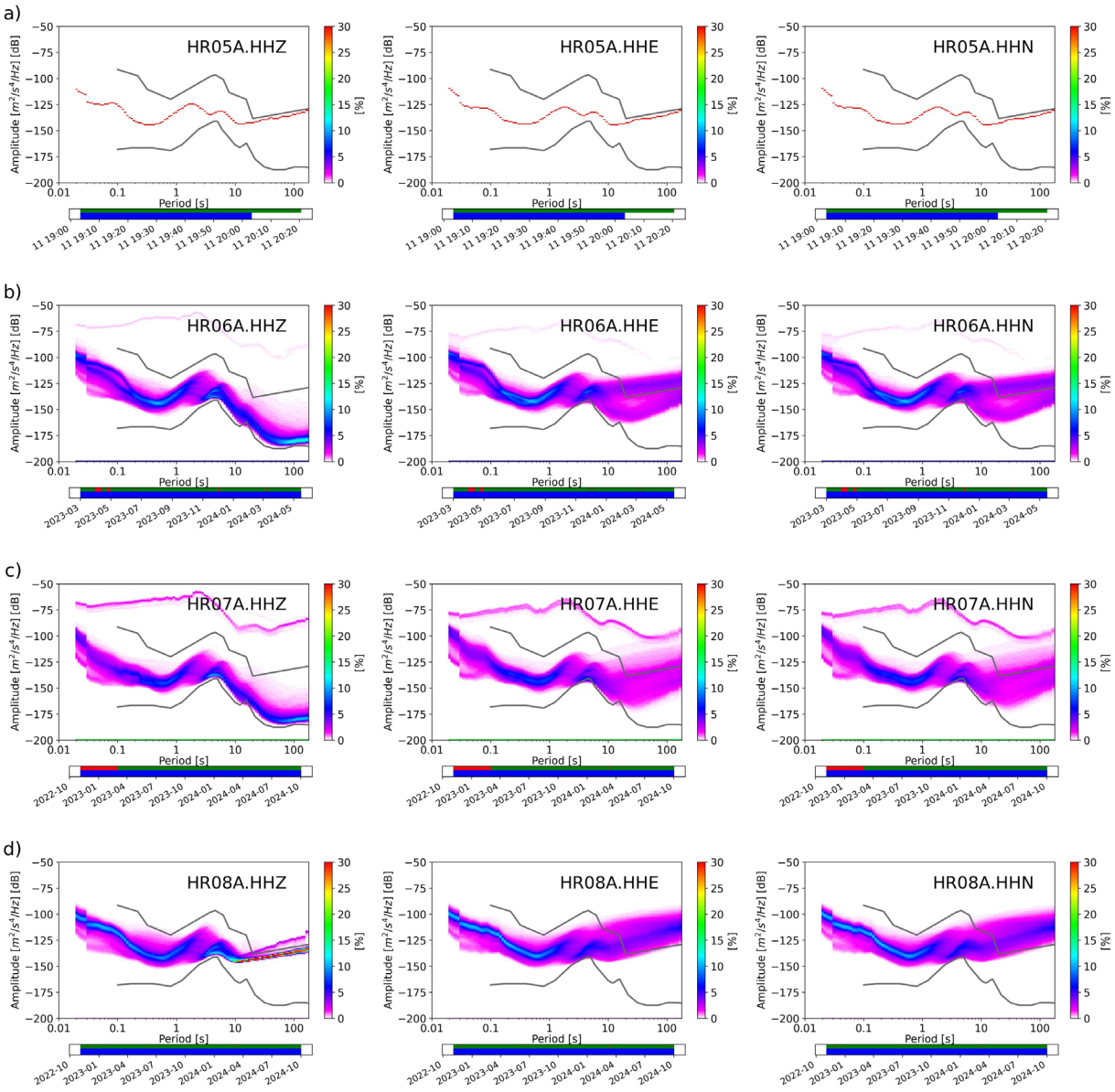

Figure A2. Probability density functions of vertical (left), E-W (middle), and N-S (right) components for four CRONOS temporary stations: (a) HR05A, (b) HR06A, (c) HR07A and (d) HR08A. The thick grey lines correspond to the NHNM and NLNM models.

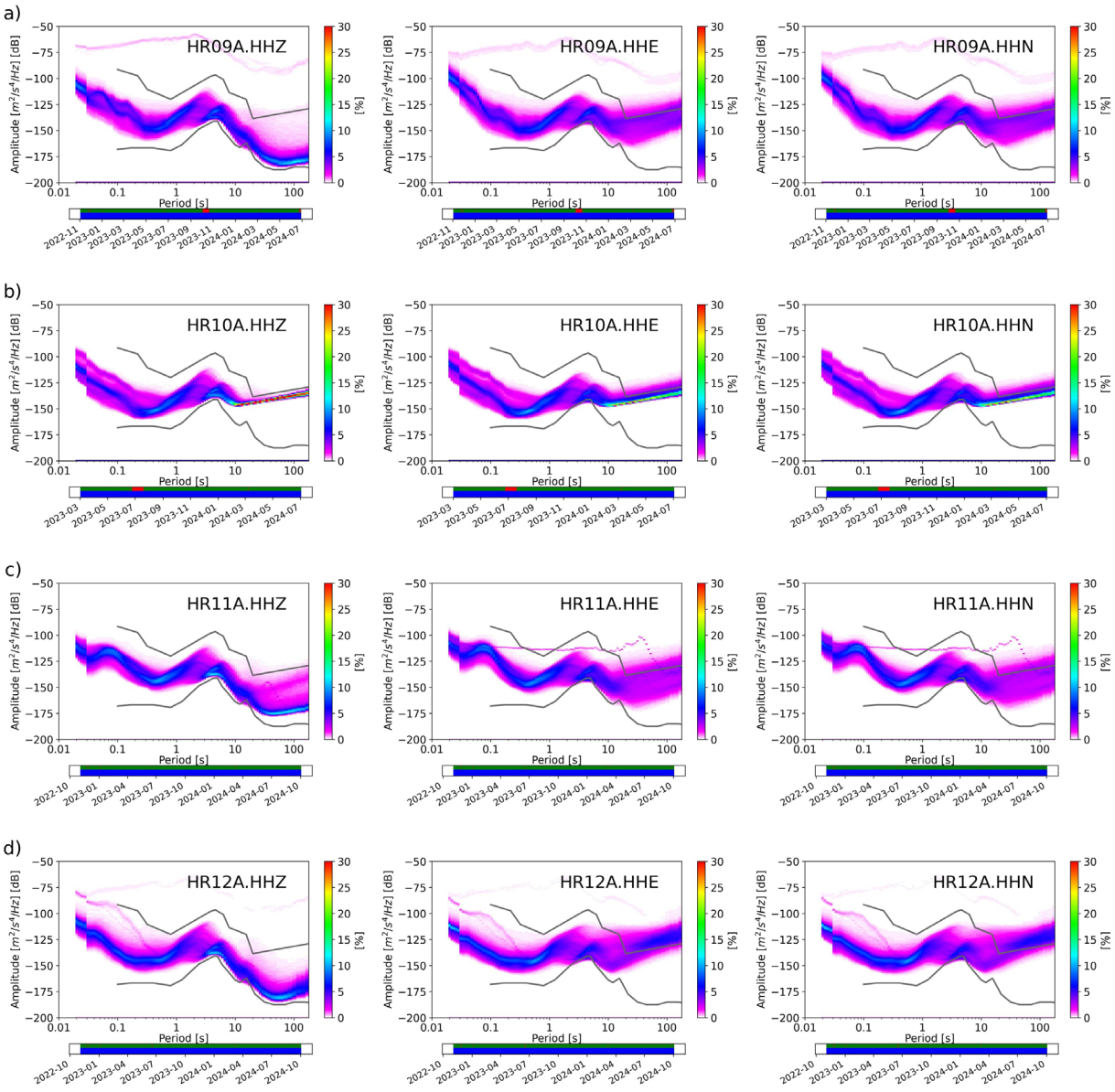

Figure A3. Probability density functions of vertical (left), E-W (middle), and N-S (right) components for four CRONOS temporary stations: (a) HR09A, (b) HR10A, (c) HR11A and (d) HR12A. The thick grey lines correspond to the NHNM and NLNM models.

***CORRESPONDING AUTHOR: Josip STIPČEVIĆ**,
Department of Geophysics, Faculty of Science, University of Zagreb, Croatia
e-mail:jstipcevic.geof@pmf.hr